C−H···Carboxylate Oxygen Hydrogen Bonding in Substrate Activation by Acyl-CoA Dehydrogenases: Synergy between the H-bonds

Robert D. Bach,* Colin Thorpe, and Olga Dmitrenko

Department of Chemistry and Biochemistry, University of Delaware, Newark, Delaware 19716

Received: January 9, 2002

Several model systems for the α-carbonyl proton abstraction reaction were studied at the DFT level to examine the role of hydrogen bonding interactions in the enzyme catalytic activity of acyl-CoA dehydrogenase. Each system contains the thioester portion of acyl-CoA ($CH_3CH_2(C{=}O)SCH_3$) a weakly basic $-COO^{\ominus}$ representing Glu376, H-donor molecules (methanol and methylformamide) with zero, one or two H-donors bound to the carbonyl oxygen of the thioester correspond to the Glu376 and FAD side-chains. Five transition structures (TS-**2**$_a$, TS-**2**$_b$, TS-**2**$_d$, TS-**2**$_{a*}$, and TS-**2**$_{b*}$) for the α-proton abstraction step and their corresponding ground state minima have been fully optimized at the B3LYP/6-31+G(d,p) level of theory. Classical activation energy barriers of 5.8, 10.4, 7.7, 9.9, and 12.3 kcal/mol have been calculated for these model systems, respectively. ChelpG, NBO charge distribution analysis in conjunction with the structural properties of the transition structures suggest their enolate-like character and the "normal" character of hydrogen bonds to the carbonyl oxygen. These energetic consequences are discussed in terms of a synergistic interplay between charge-augmented (ionic) and neutral ("normal") H-bonds. These interactions serve to disperse this negative charge not only in the ground state but also in the TS, thereby strengthening the internal H-bonds along the entire reaction coordinate. An additional unanticipated insight, with the identification of a strong ionic C−H···carboxylate-oxygen H-bond along the reaction coordinate provides an activating influence for the α-proton abstraction. The ionic C−H···$^{\ominus}$OOC H-bond identified here would not only orient the general base prior to proton abstraction, but also transfers electron density to the developing enolate anion along the reaction coordinate. This strengthens the H-bonds to the thioester carbonyl oxygen that prove so critical in the acidification of the α-proton and lowers the energy of the transition state for enolization. The correlation between the reaction endothermicity, barrier height and location of the transition state along the reaction coordinate is consistent with the classical Hammond postulate. Solvent modeling performed with the COSMO//B3LYP/6-31+G(d,p) method confirms the important role of desolvation of the carboxylate anion prior to the α-proton abstraction step.

1. Introduction

Acyl-CoA dehydrogenase catalyzes the two-electron oxidation of a broad range of fatty acids with the conversion of acyl-CoA thioesters to their corresponding α, *β*-enoyl-CoA products. Dehydrogenation occurs by the breakage of two kinetically stable C−H bonds of the substrate introducing a carbon−carbon double bond as shown in Scheme 1.[1] The first C−H bond breaking requires chemical activation of an adjacent thioester functionality and abstraction of hydrogen as H^+ by the weakly basic Glu376-$COO^{\ominus}$ with, what is presumed to be, a concomitant expulsion of a *β*-hydride that is transferred to N-5 of the FAD isoalloxazine ring. Strong support for this concerted pathway, as opposed to the intervention of a discrete intermediate such as a delocalized α-carbanion, comes from kinetic isotope effect (KIE) studies.[1]

Scheme 1 is, at best, a gross oversimplification and a number of its critical aspects, including how GLU376 functions as a general base,[1b−d] the *precise* role of desolvation in catalysis,[1b,c] the polarization of the substrate carbonyl group by H-bonding,[1b−d] and finally the mode by which reducing equivalents are transferred to the flavin,[1a,1b,2] remain cryptic. This is because a rate-limiting isomerization of the encounter complex precedes the chemical steps with good substrates, and the reaction is not amenable to conventional linear free energy analysis.[1b,1c,1e] Thus,

SCHEME 1

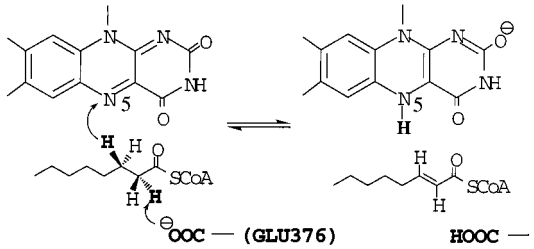

we seek insight from computational approaches. It is not our intent to represent the enzyme itself, but rather to provide a model system that serves to describe the intrinsic gas-phase behavior of and how its surrounding hydrogen bonding interactions affect the activation barrier for α-carbonyl proton removal.

We initially address the mechanism of α-proton abstraction without concern for the concomitant transfer of a hydride equivalent to the flavin. Computation of the full dehydrogenation reaction, involving the entire isoalloxazine and a minimum suite of ancillary atoms would require extensive computing resources. Further, there is unequivocal experimental evidence for uncoupling α-proton abstraction from reduction of the flavin ring using 3-substituted redox-inactive thioester analogues.[1b,1d] For example, 3-thiaoctanoyl-CoA cannot transfer a hydride ion, has a

10.1021/jp020029k CCC: $22.00
Published on Web 03/20/2002

TABLE 1: Calculated Proton Affinities (PA, kcal/mol) of Anionic Bases and Enolate Intermediates and Available Experimental Deprotonation Energies (kcal/mol)[a]

anion	B3LYP/6-31+G(d,p)	G2	exp $\Delta H°$
HO	395.7 [387.4][b]	388.6 [388.3]	390.7
HCOO	348.1 [339.4][b]	342.1 [341.9]	345.3
CH_3COO	352.9 [343.6][b]	345.7 [345.6]	348.1
$CH_3COO{\cdot}H_2O$	341.7		
(CHO)N**H**)$CH_2CH_2CH_2COO$[c](all trans)	345.1		
$CH_2(C{=}O)H$	372.4 [363.6][b]	366.2 [365.9]	365.8
$CH_3CH(C{=}O)CH_3$	375.4 (374.8)[d] [366.7][b]	368.3 [368.0]	
$HOCH(C{=}O)CH_3$	369.9 [362.0][b]		
$CH_3CH(C{=}O)SCH_3$ (I)	369.2 [359.8][b]	362.7 [362.7]	
$CH_3CH_2CH(C{=}O)SCH_3$ (II)	367.9		
$CH_3CH(C{=}O)SCH_3{\cdot}2H_2O$	351.5		
$CH_3CH(C{=}O)SCH_3{\cdot}CH_3O$**H**	360.0 [350.6][b]		
$CH_3CH(C{=}O)SCH_3{\cdot}$**H**NCH3(C=O)H	354.3 [344.9][b]		
$CH_3CH(C{=}O)SCH_3{\cdot}(CH_3O$**H**, **H**NCH3(C=O)H)	345.3		
$CH_3CH_2CH(C{=}O)SCH_3{\cdot}CH_3O$**H**	359.1 [349.7][b]		
$HSCH(C{=}O)SCH_3{\cdot}(CH_3O$**H**, **H**NCH3(C=O)H)	336.4		

[a] NIST *Standard Reference Database,* Number 69, Feb. 2000 (http://webbook.nist.gov/chemistry.). [b] Thermal corrections to enthalpies are obtained from the geometries and frequencies calculated at the B3LYP/6-31+G(d,p) level. [c]Glu model as in system **d**. [d] PA calculated at QCISD(T)//QCISD/6-31G(d). [e] The numbers in brackets are based upon enthalpies at 298.15° K.

free p*K* of about 16, and yet is deprotonated essentially completely when bound to the active site of the acyl-CoA dehydrogenase at pH = 7.[1b,3]

In addition to the generally accepted elevation of the p*K* of GLU376 by desolvation,[1b,1c] a critical aspect of the stabilization of the TS involves two hydrogen bonds directed toward the thioester carbonyl group.[1b,1d] A peptide chain N−H group provides one H-bond, and is thus difficult to manipulate experimentally. A second is from the 2′-OH of the ribityl moiety of FAD. Replacement with the 2-deoxy-FAD analogue slows the reductive half-reaction (Scheme 1) by about 10^7-fold and prevents the enolization of redox-inactive 3-thiaoctanoyl-CoA.

Our computational approaches are consistent with the well-established critical role played by H-bonds to the substrate carbonyl group.[4] However, they provide an additional insight, with the identification of a strong ionic C−H···carboxylate-oxygen H-bond (C−H···$^{\ominus}$OOC-) along the reaction coordinate. H-bonds between weak carbon acids and carbonyl groups (C−H···O=C bonds) have only recently been recognized as important, if under-appreciated, stabilizing interactions in protein crystallography and molecular recognition[5] and as a directing influence in organic reaction mechanisms. Their role in the deprotonation of carbon acids by carboxylate bases in enzymes has not, to our knowledge, been emphasized previously. Additionally, reactions involving CoA thioesters are widespread in enzymology[4d] and thus density functional theory calculations with relatively flexible basis sets may have broad applicability. Our primary goal is to characterize energetically the intrinsic gas-phase stabilizing influence of both types of H-bonding interactions on the activation barrier for the key α-proton abstraction step.

2. Computational Methods

Ab initio molecular orbital calculations were performed with the Gaussian 98 program.[6] The Becke three-parameter hybrid functional combined with the Lee, Yang, and Parr (LYP)[7] correlation functional, denoted B3LYP,[8] was employed in the calculations using density functional theory (DFT). In all calculations, we used 6-31G(d), 6-31+G(d,p) or 6-311+G(3df,-2p) basis sets.[9] In some cases, for smaller molecules, calculations at the QCISD(T)//QCISD[10] and G2[11] levels of theory were performed. The stationary points on the potential energy surfaces were characterized by calculations of vibrational frequencies at the B3LYP/6-31+G(d,p) level. The partial charges were calculated using the NBO and CHelpG methods[12] implemented in the Gaussian 98 program. Corrections for solvation were made using polarizable conductor COSMO model calculations.[13] Proton affinities (PA) at the G2 level for the selected anions are in excellent agreement with experiment; relative PAs at B3LYP/6-31+G(d,p) are consistent with the G2 results (Table 1).

For a design of the appropriate models for the GLU376 base-catalyzed α-proton abstraction from CoA, the X-ray structure of the medium chain acyl-CoA dehydrogenase (MCAD) active site was used as a geometry reference. The X-ray structures of the medium-chain acyl-CoA[14a] dehydrogenase and related butyryl-CoA[14b] dehydrogenase (BCAD) were obtained from the Protein Data Bank.[14c] Thioester **I** ($CH_3CH_2(C{=}O)SCH_3$ was chosen to model the CoA substrate in the smaller systems (**a**, **b**, and **c**). The desolvated catalytic base in GLU376 is represented by acetate ion ($CH_3COO^{\ominus}$). The H-bond donors to the thioester carbonyl group are methanol (corresponding to the 2′-OH of the FAD) and the N−**H** of methylformamide (mimicking the peptide N−H in GLU376).

Thioester **II** $CH_3CH_2CH_2(C{=}O)SCH_3$), with an additional methylene group, was used in extended model system **d**. The active site base ($-COO^{\ominus}$) and the amide hydrogen donor (**H**−N<) are combined in a single molecule (H(C=O)−N**H**−CH_2-$CH_2CH_2COO^{\ominus}$)) which more closely resembles the GLU376 side chain. Two additional extended model systems (**a***, **b***) use thioester **II** as the substrate but have the N**H** and H(C=O) groups transposed H(C=O)−CH(NH**H**)$CH_2CH_2COO^{\ominus}$)) to provide a comparison of the catalytic effect of the less acidic amine versus an amide as a H-bond donor in the TS for α-proton abstraction. Extended models **a*** and **b*** correspond to the above smaller models (**a** and **b**) with and without the second H-bond donor, methanol. All models bear a net negative charge. Optimization of all structures used the Berny algorithm.[6b] The keyword MODREDUNDANT[6a] was used in the more complex structures. Additional bond distances (e.g., H-bonding interactions) were included as explicit variables when they typically were over 2 Å. Some additional bond angles, not treated specifically, and especially dihedral angles involving H-bonds were added between the four heavy atoms (C=O···H···N−C)

omitting the hydrogen atom. This dampens the displacements cutting down on wagging and bending motions and typically reduces the number of gradient cycles by up to one-half. Throughout the text, bond lengths are in Ångstroms and bond angles are in degrees.

3. Results and Discussion

Although in the past thirty years theoretical studies have covered most of the basic reactions used by the experimental community, transition structures for the abstraction of a proton adjacent to a carbonyl group is an area that has received less attention. There have been a series of high level systematic studies[15] on identity-reaction proton transfers from the weak carbon acid, acetaldehyde. In the transition state for proton transfer from acetaldehyde-to-acetaldehyde enolate the pK_a of each partner is perfectly matched and the TS has the proton in the middle of the two carbon atoms (C···H···C). The principle of microscopic reversibility requires the TS to be symmetrical in that the proton is equidistant between the two fragments. It was not until 1996 that Perakyla reported the first attempts at the Hartree−Fock level to describe bimolecular unsymmetrical TSs for α-proton abstraction from the simplest carbonyl derivative, acetaldehyde.[16a] There have been no examples reported of transition structures for the key α-proton abstraction step at a correlated level of theory. When the p*K*s of the reacting partners are mismatched, the reaction can either be highly exothermic or endothermic. An exothermic reaction, with an early TS, often occurs without a discernible barrier! Ion cyclotron resonance (ICR) studies have established that gas-phase proton transfers from a neutral to an anion can occur without barrier.[17a] To a first approximation, the relative proton affinities (PAs) of the reactants (Table 1) give a good indication of the position of the proton abstraction TS along the reaction coordinate.[18] As a standard protocol, we use the PA of the conjugate base as a guide to the position of TS along the reaction coordinate.

Electronic and Structural Features of the Thioenolate Anion. Reactions involving proton abstraction from a weak carbon acid by what is typically a weak base are usually endothermic. Thus, the problem with exothermic reactions involving strong bases[18] can be mitigated in part by using a weaker base such as formate or acetate anion to get a closer match of the p*K*s. However, in this case the reaction can become endothermic with a late TS and often a product cluster does not exist as a stationary point at a correlated level of theory. Kollman et al.[19] and Karplus et al.[20] have studied this α-proton abstraction mechanism using α-hydroxyacetone derivatives as triosephosphate isomerase (TIM) model substrates. In a more recent study Cui and Karplus[20a] have applied the QM/MM method to TIM catalyzed reactions using AM1 parameters optimized for TIM reactions based upon B3LYP/6-31+G(d,p) gas-phase results. Houk[21] has also recently reported a study on α-deprotonation of a series of rather large ketones at the HF/6-31G(d) level. A model study[22] on citrate synthase involving proton abstraction by acetate anion from methythioacetate (representing the catalytic base Asp375 and acyl-CoA) has also been reported

$$CH_3COO^{\ominus} + CH_3C{=}OSCH_3 \rightarrow CH_3COOH + CH_2C{=}OSCH_3^{\ominus} \quad (1)$$

A model study by Mulholland et al.[22c] on citrate synthase (CS), also used Reaction 1 as a model. The QM calculations reported were at the MP2/6-31G(d) and HF/6-31G(d) levels of theory. The QM/MM surface gives a measure of the stabilization provided by the surrounding environment, and the energy profile calculated indicates an increase in the reaction barrier in comparison with the QM system alone.

As anticipated on the basis of relative PAs, at an electron correlated level, reaction 1 reverses, and the carboxylic acid proton migrates back to the thioester enolate affording starting materials. The PA of thioester **I** (362.7 kcal/mol, G2) is also sufficiently greater than that of acetate anion (345.7 kcal/mol, Table 1) that the acetate anion is too weakly basic to abstract a proton in the absence of some external stabilizing influence. However, if the relative energy of the product cluster can be lowered by the hydrogen bonding interaction of such hydrogen donors as alcohols or amides, a product cluster can exist as a minimum and a TS can, in principle, be located.

Because the first step for acyl-CoA dehydrogenase involves an α-proton abstraction, we have examined the electronic structure of the enolate derived from α-proton abstraction of model thioester **I** and the question of the validity of the classical resonance structures for model thioester **I**, its enol form and its enolate anion. Classical resonance theory suggests that α-C−H abstraction from thioester **I** would give rise to a thioenolate anion that is usually described as a delocalized resonance structure where the negative charge is clearly associated with the electronegative oxygen atom. It is generally assumed by the experimental community that the C−C bond shortens and the C−O bond in the TS lengthens for α-proton abstraction from a thioester (or ketone). Hence, *it is presumed* that the increase in electron density at the carbonyl oxygen gives rise to stronger hydrogen bonds to the carbonyl oxygen, which ultimately reduces the activation barrier for α-proton abstraction.

In thioester **I** (Figure 1) the developing negative charge on oxygen is only increased by −0.20 electrons upon going from the thioester to the thioenolate form. As anticipated, the minimal change in charge on oxygen is consistent with a very small increase in the C═O bond length (0.04 Å), whereas the large increase in charge at the sp^2 carbon does give C−C bond shortening. The bulk of the negative charge resides on the carbon fragment (ΔQ CH_3CH = −0.40) and the SCH_3 fragment (ΔQ SCH_3 = −0.34). The total "−1" charge is distributed over the entire molecule, and the change of the C−O bond length is not significantly influenced by enolate formation. The high degree of carbonyl character maintained in the thioenolate (C═O = 1.26 Å) is a consequence of the fact that in this case the thioester structure **I** is 20 kcal/mol more stable than its enol form reflecting the greater thermodynamic stability of a carbonyl double bond (C═O) versus a carbon−carbon double bond (C═C). Thus, despite the greater electronegativity of oxygen versus carbon, much of the negative charge remains on the carbon fragment in order to maintain the carbonyl character of the enolate. The carbonyl group is already highly polarized toward oxygen in the ground state so little change is anticipated in the TS. A more fundamental question is how does the charge shift in the TS for αC−H abstraction and is this rather simple picture altered by αC−H activation by hydrogen bonding interactions?

α-Proton Abstraction from the Thioester Model I and the Synergistic Assistance of H-Bonding Interactions to Carbonyl Oxygen. *Models a, b, and c*. Enzymologists are particularly interested in how enzymes achieve catalysis of reactions that involve a weakly acidic C−H functionality. To investigate the role of H-bonding and characterize the transition structures

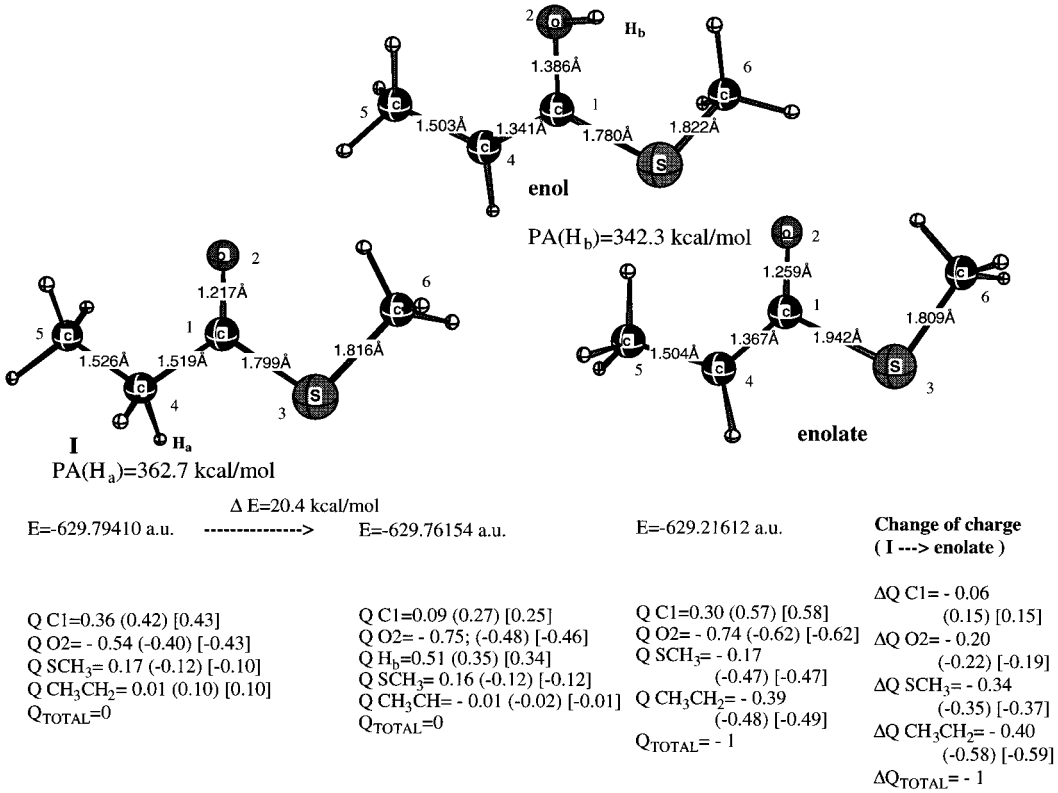

Figure 1. Geometry of thioester **I** ($CH_3CH_2(C{=}O)SCH_3$), its enol and enolate optimized at the QCISD/6-31G(d) level of theory. Energies are at the G2 level. The charge distributions were estimated using a NBO analysis at MP2/6-31+G(d,p) on MP2/6-31G(d) optimized geometries. The numbers in parentheses are developing charges calculated by CHelpG (MP2/6-31+G(d,p)) on QCISD/6-31G(d) geometries. The numbers in brackets are ChelpG charges at the B3LYP/6-31+G(d,p) level of theory.

SCHEME 2

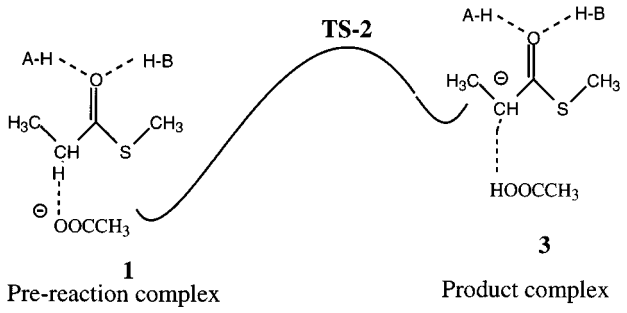

a - A-H = CH_3O-H and B-H = H-NCH_3(C=O)H
b - one H-donor, B-H = H-NCH_3(C=O)H
c - no H-donors

for the α-proton abstraction step in acyl-CoA dehydrogenase, we have performed calculations on three model systems, **a**, **b**, and **c** (Scheme 2), that contain two, one, and zero hydrogen bonds to the carbonyl oxygen of model thioester **I**, respectively.

Model system **a** consists of the thioester portion of acyl-CoA, acetate anion, methylformamide (representing GLU376), and methanol (corresponding to the 2′-OH of the FAD). Figure 2 depicts five stages along the reaction coordinate for the proton abstraction step in model systems **a**, **b**, and **c**. When both H-bonding donors ($CH_3O\mathbf{H}$ and $\mathbf{H}NCH_3(C{=}O)H$) are involved in hydrogen bonding to the carbonyl oxygen, curve **a** is realized.

Reactant-cluster $\mathbf{1}_\mathbf{a}$ (see below) comprising three H-bonding interactions, including the ionic C−H···$^{\ominus}$OOC-hydrogen bond, is 29 kcal/mol lower in energy than its isolated reactants. This very large charge-augmented stabilization energy may be conceptually dissected as shown in Figure 3.

If the two H-bonds to the carbonyl oxygen are formed first, an aggregate stabilization energy of 8.7 kcal/mol is predicted (typical for neutral species of this type). However, initial formation of the CH···carboxylate H-bond yields −11.6 kcal/mol of stabilization. This value is understandably larger than the 1 to 4 kcal/mol calculated for a number of CH···neutral oxygen species[5d,23] (C−H···O=C) because this H-bond is between an electron deficient α-carbonyl proton and the carboxylate anion. Obviously, it is immaterial which interaction forms first upon desolvation of the active site, but note the strong synergy between them. Thus, the overall stabilization of 29 kcal/mol is 9 kcal/mol more (nonadditive effect[22c]) than the sum of their individual contributions (−8.7 and −11.6 kcal/mol, Figure 3). This striking charge-augmented stabilization of the reactant cluster is then reapportioned and strengthened along the remainder of the reaction coordinate as the initial ionic H-bond (C−H···O−C) is transformed into proton transfer to the carboxylate base.

The effect of H-bond donors on the relative stability of the enolate ion resulting from α-proton abstraction can be estimated from their respective proton affinities. The decrease of α-proton affinity derived from the **H**-N residue ($PA_{CH3CH(C=O)SCH3} - PA_{CH3CH(C=O)SCH3\cdot\mathbf{H}NCH3(C=O)H} = 14.9$ kcal/mol) is surprisingly larger than the **H**−O hydrogen bond ($PA_{CH3CH(C=O)SCH3} - PA_{CH3CH(C=O)SCH3\cdot\mathbf{H}OCH3} = 9.2$ kcal/mol) based upon PA values given in Table 1. The combined decrease in the α-proton affinity derived from the H-bonded alcohol and amide molecules is considerably larger than that of two H-bonded water molecules, (23.9 vs 17.7 kcal/mol, Table 1). The efficacy of these two model H-donors is further demonstrated by a comparison with the experimental and theoretical complexation energies of methanol with water; $CH_3OH + H_2O \leftrightarrows CH_3O^{\ominus}\cdot H_2O$ ($\Delta H° = -23.9$ and -23.0 kcal/mol, respectively).[17c] Thus, the role of

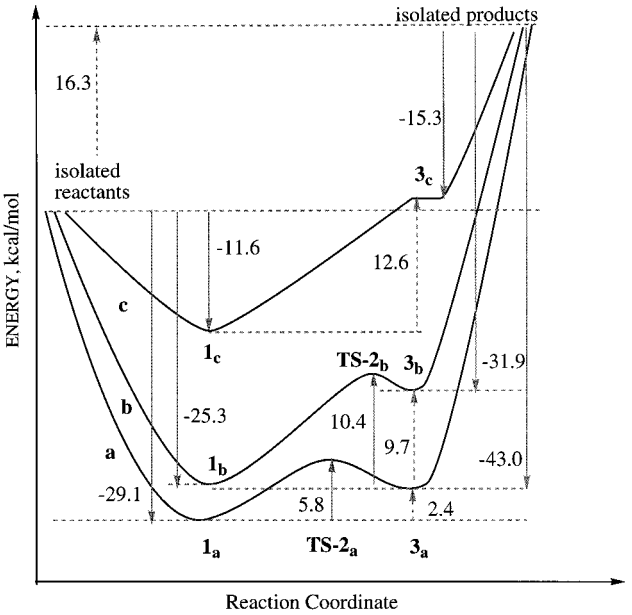

Figure 2. B3LYP/6-31+G(d,p) energy diagram for α-proton abstraction from model thioester **I** ($CH_3CH_2(C{=}O)SCH_3$) by acetate anion. The lower curve (**a**) represents reaction energetics along the reaction coordinate for the system with two H-donors (A−H = CH3O−**H** and B−H = **H**−NCH3(C=O)H). Curve **b** corresponds to the model system with one H-donor, methylformamide. The upper curve (**c**) is for α-proton abstraction without any H-bond donors. TS-**2a** and TS-**2b** are both first-order saddle points; no product minimum (or TS) was located for curve **c**. The energy of the product cluster was estimated to be 12.6 kcal/mol above minimum **1c** (in the product cluster **3c**, CH3CH2(C=O)SCH3·CH3CO**OH**, the |O−H| = 1.01 Å bond was fixed during optimization).

the carbonyl H-bonds is to lower the pK_a of the α-proton as evidenced by the dramatic stabilization of the conjugate base of the pre-reaction complex.

The classical activation barrier for α-proton abstraction from $CH_3CH(C{=}O)SCH_3{\cdot}(CH_3O\mathbf{H}$, **H**NCH3(C=O)H) (**1a**) by $CH_3COO^{\ominus}$ is 5.8 kcal/mol (**TS-2a**, $\Delta E^{\neq}$ 7.0 kcal/mol MP2//B3LYP/6-31+G(d,p) level) and the product thioenolate cluster **3a** is only ΔE_{reac} = 2.4 kcal/mol (3.3 kcal/mol at the MP2//B3LYP/6-31+G(d,p)) less stable than reactant cluster **1a** (Figure 4). Extensive ICR studies by Brauman and co-workers have shown that small gas phase barriers may result when there is significant delocalization especially as the reaction approaches thermoneutrality.[17a]

The α-proton is more than one-half transferred in TS-**2a**. The other changes in geometry on going from reactant cluster **1a** to TS-**2a** are minimal with the exception of the carbonyl oxygen H-bond distances (−H···O=C) that gradually shorten as electron density is transferred from the carboxylate base to the thioester fragment along the reaction coordinate. These two carbonyl H-bonding distances are 1.91 and 2.15 Å in reactant cluster **1a**, but are reduced to 1.74 and 1.84 Å in product cluster **3a** *as a consequence of the increase in charge on the thioenolate fragment* (Table 2 and Table 3).

The molecular architecture of pre-reaction cluster **1a** has the H-bonded carboxylate base ideally poised to receive the proton in the TS with minimal heavy atom motion as also evidenced by the very small $\Delta S^{\neq}$ (Table 4).

The reaction vectors of the single imaginary frequency is essentially comprised of the proton transfer with very little contribution of hydrogen bond movement involving the carbonyl oxygen. The thioester fragment in **1a** has a charge of 0.017 but in **TS-2a** it carries a charge of −0.46. The increase in negative

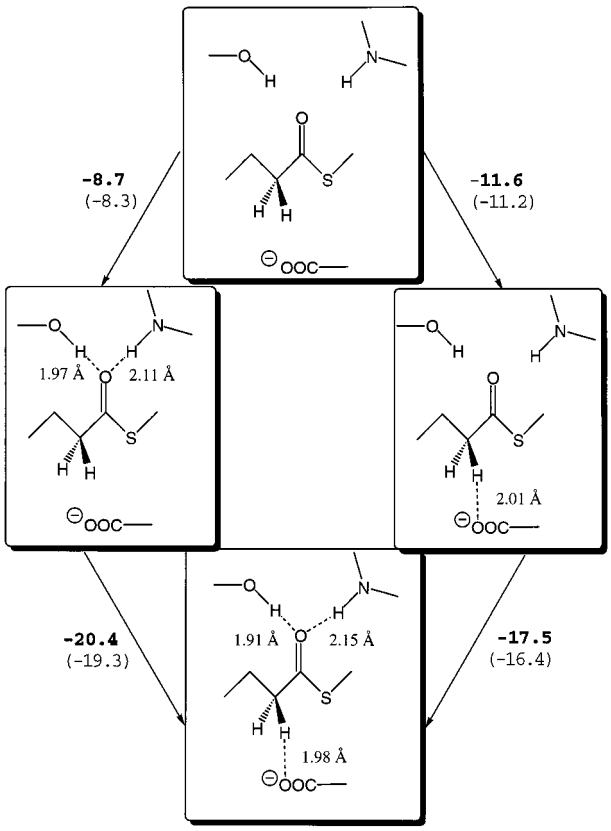

Figure 3. Schematic representation of the H-bonding stabilization energy (kcal/mol) in the reactant cluster ($CH_3COO^{\ominus}\cdots CH_3CH_2(C{=}O)SCH_3{\cdot}(CH_3O\mathbf{H}$, **H**NCH3(C=O)H)) that can be distributed in two different ways depending upon the sequencing of H-bonding interactions (see text for more details). The stabilization energies shown in bold are at the B3LYP/6-31+G(d,p) level, whereas numbers in parentheses are refined by single point B3LYP/6-311+G(3df,2p)//6-31+G(d,p) calculations.

TABLE 2: ChelpG Charges on Selected Functional Units of Model a (MP2/6-31+G(d,p)//B3LYP/6-31+G(d,p))[c]

	$CH_3OO(H_t)$	$CH_3CH(H_t)(C{=}O)SCH_3$	H-donors	H_a (in methanol)	H_b (in methylformamide)
1a	−0.877	0.017[a]	−0.141	0.415	0.201
	[−0.863][b]	[0.023]	[−0.159]	[0.411]	[0.193]
TS-2a	−0.363[a]	−0.458	−0.179	0.386	0.165
	[−0.365]	[−0.448]	[−0.187]	[0.381]	[0.154]
3a	−0.154[a]	−0.458	−0.389	0.265	0.047
	[−0.164]	[−0.450]	[−0.386]	[0.268]	[0.046]

[a] The charge on hydrogen H_t is included. [b] The numbers in brackets are ChelpG charges at the B3LYP/6-31+G(d,p) level. [c] The charge evolution along the reaction coordinate on selected atoms and functional parts of the model (see Figure S1 in the Supporting Information for more details).

charge on the carbonyl oxygen going from **1a** to **TS-2a** is only −0.08 (or 17% of the charge transferred to the thioester fragment, Table 3). This is consistent with retention of a high degree of carbonyl character in **TS-2a**; C=O = 1.26 Å. Even when the product cluster **3a** is examined, the charge on the thioenolate oxygen atom is still only −0.10. *Thus negative charge is spread over the entire thioester fragment* during enolization (Table 3) and an adequate description of the electrostatic and resonance aspects of α-proton removal should not focus unduly on the increase in electron density at the carbonyl oxygen. H-bond distances between heteroatoms: 3.14 and 2.89 Å in **1a**; 2.94 and 2.79 Å in **TS-2a**; 2.86 and 2.72 in **3a** for N···O and O···O, respectively are far greater than the

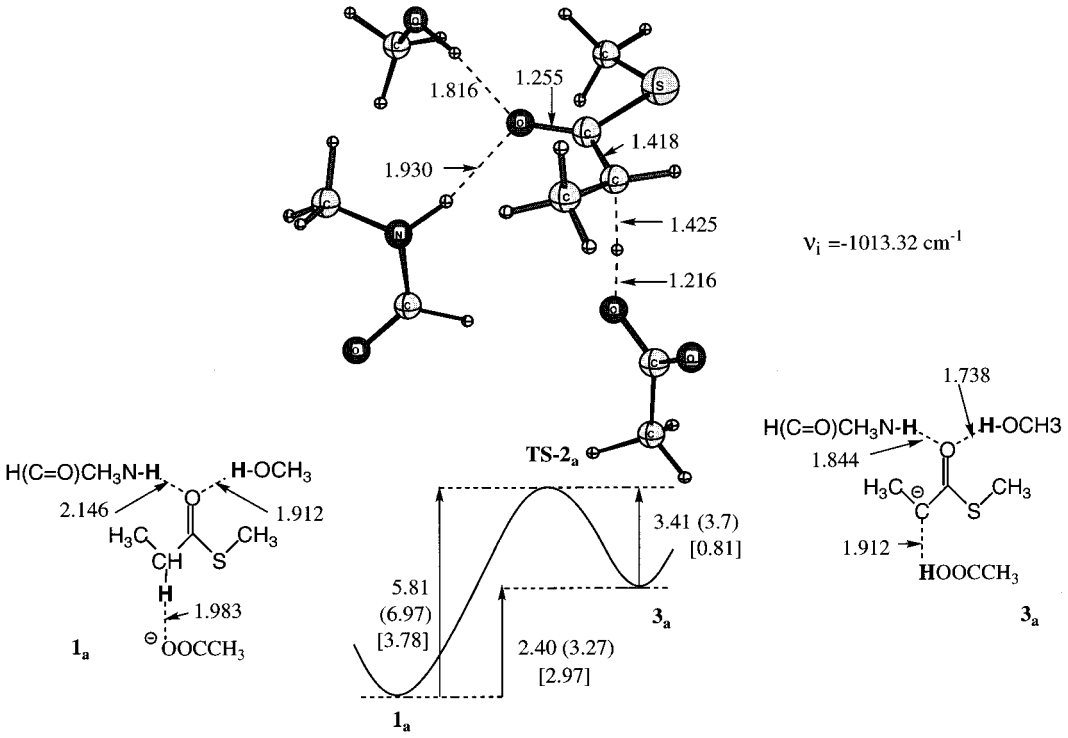

Figure 4. Fully optimized transition structure and relative energies (kcal/mol) of the optimized pre-reaction cluster, TS and product cluster of model system **a** ($CH_3COO^{\ominus}\cdots CH_3CH\mathbf{H}(C{=}O)SCH_3\cdot(CH_3O\mathbf{H}, \mathbf{H}NCH3(C{=}O)H)$) at the B3LYP/6-31+G(d,p) level of theory. Numbers in parentheses correspond to MP2//B3LYP/6-31+G(d,p) calculations. Numbers in brackets are based upon free energy data. To prevent the complexation of $CH_3COO^{\ominus}$ and **H**NCH3(C=O)H, reactant cluster **1$_a$** has been optimized with dihedral angle N−H..O=C frozen to 165.85° as calculated in the optimized cluster without the $CH_3COO^{\ominus}$ base.

TABLE 3: ChelpG Charges and Distribution of the Developing Negative Charge on Selected Atoms and Groups in the Thioester Fragment of Model a (density = MP2, 6-31+G(d,p)[c]

	$CH_3CH(H_t)$	C	O	SCH_3
1$_a$	0.118[a]	0.384	−0.337	−0.148
TS-2$_a$	−0.189 (64%)[b]	0.385 (0%)[b]	−0.415 (17%)[b]	−0.240 (19%)[b]
3$_a$	−0.184	0.179	−0.098	−0.356

[a] The charge on hydrogen H_t is included. [b] $n\% = 100*(q_I - q_R)/(Q_{thio,TS} - Q_{thio,R})$, where $Q_{thio,TS} = -0.475$ is negative charge transferred to thioester unit in the transition state. Analogous calculations based upon an NBO analysis (B3LYP/6-31+G(d,p), see Supplementary Information) resulted in a similar charge distribution: 65% of $Q_{thio,TS} = -0.653$ is developing on $CH_3CH(H_t)$, 7% on C, 15% on O and 13% on SCH_3. [c] The geometries of the three reaction stages of model **a** were optimized at the B3LYP/6-31+G(d,p) level of theory.

TABLE 4: Thermochemical Data at the B3LYP/6-31+G(d,p) Level of Theory[a]

reaction	$\Delta E^{\neq}$, kcal/mol	$\Delta(E + ZPE)^{\neq}$, kcal/mol	$\Delta S^{\neq}$, e.u.	$\Delta G^{\neq}$, kcal/mol	imaginary frequency, cm^{-1}
1$_a$→ TS-2a	5.8	2.8	−4.8	3.8	−1013.3
1$_b$→ TS-2b	10.4	7.2	−3.6	7.9	−816.1
1$_d$→ TS-2d	7.7	5.0	−1.2	5.3	−1124.4
1$_a$*→ TS-2a*	9.9	7.2	−10.1	9.6	−1028.1
1$_b$*→ TS-2b*	12.3	9.4	−5.7	10.7	−748.5

[a] Zero point energies and statistical mechanical contributions to the entropy are obtained from the geometries and frequencies calculated at the B3LYP/6-31+G(d,p) level; for the total energies and other details, see Table S2 in Supplementary Information.

2.5 Å required of a special type of short-strong hydrogen bond. To our knowledge, **TS-2$_a$** is the first example of a first-order saddle point for proton abstraction adjacent to a carbonyl group performed at a correlated level.

In HF/6-31+G(d) studies on the relative models designed to mimic citrate synthase,[22c] it has been noted that the sulfur atom of the thioester may be of importance for stabilizing the enolate form by charge acceptance. Our results also show a gradual increase in charge on the $-SCH_3$ group thereby supporting the polarization concept. Thioester **I** itself is more acidic than the corresponding oxygen ester as indicated by a PA difference of 6.2 kcal/mol (Table 1) in consonance with the greater polarizability of sulfur versus oxygen. Additionally, substitution of the β-methyl group in the thioester (with methanol and methylformamide H-bonded to its oxygen) for a SH group ($HSCH(C{=}O)SCH_3\cdot(CH_3O\mathbf{H}, \mathbf{H}NCH_3(C{=}O)H$, Table 1) reduces the proton affinity (PA) of the complex by 9 kcal/mol which, in principle, should make the α-proton abstraction more feasible.

Examination of the structural and electronic changes for **TS-2$_a$** versus reactant complex **1$_a$** (Figure 4 and Table 3) reveals that they are quite similar to that of thioenolate vs thioester calculated by more accurate QCISD and G2 methods (Figure 1). Thus, the present calculations provide convincing evidence that *the transition state has enolate-like character*, albeit with most of the charge residing on the thioester backbone itself. Gas-phase ICR experiments suggest that the effects of charge-transfer compete with the effects of rehybridization and charge delocalization such that these effects tend to cancel each other out.[17a]

Calculations with only one H-bond to the carbonyl oxygen ($\mathbf{H}NCH_3(C{=}O)H$) mimic removal of the 2′-OH-ribityl H-bond[1d] (curve **b** in Figure 2) and show that the barrier (**TS-2$_b$**, see Figure 5**)** is raised to 10.4 kcal/mol (corresponding to a 10^3-fold reduction in enolization rate). These data should be compared with experimental data on the 2-deoxy-ribityl derivative where a rate reduction of ≈10^7 was reported.[1b]

In comparison, enolization of the substrate in the absence of both carbonyl H-bonds (curve **c**, Figure 2) is highly endothermic

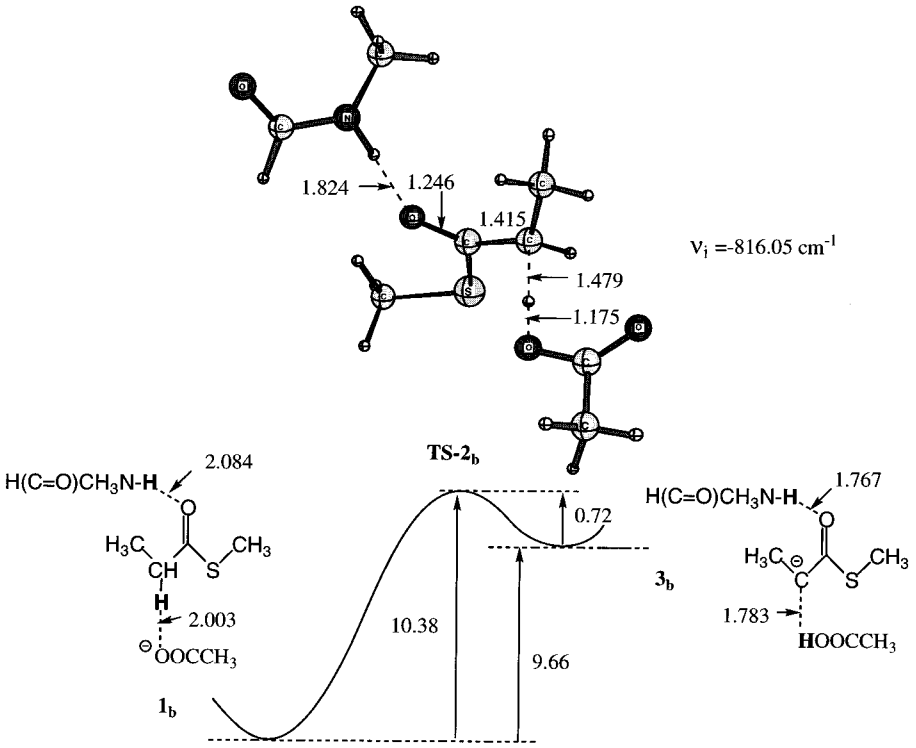

Figure 5. Fully optimized transition structure and relative energies (kcal/mol) of the optimized pre-reaction cluster, TS and product cluster of model system **b** ($CH_3COO^{\ominus}\cdots CH_3CH\mathbf{H}(C{=}O)SCH_3\cdot\mathbf{H}NCH3(C{=}O)H$) at the B3LYP/6-31+G(d,p) level of theory.

(with an estimated barrier of 13 kcal/mol).[24] Here, multiple approaches failed to produce a bona fide transition state (first-order saddle point).[24] The observed tendency of the barrier to increase with an increase of the reaction endothermicity is an evident example of the implementation of the Hammond postulate which works in cases where the ionization potential correlates with bond strengths.[25] A reaction that is highly endothermic (exothermic) is expected to have a high (low) activation barrier and late (early) transition state. A simplified view, consistent with the Hammond postulate that explains the energy diagrams shown in Figure 2 and provides an explanation for the lack of the TS and product in the model **c**, is given in Figure 6.

Our results suggest a critical role of H-bonding synergism in the proton abstraction step. The H-bonds to the thioester carbonyl oxygen atom first act to reduce the reaction endothermicity from 16.3 to 2.4 kcal/mol (Figure 2, curve **a**) due to their larger energetic contribution to the product cluster. In accord with the Hammond postulate and the increased stabilization of the TS versus the pre-reaction complex, a lowering of the reaction barrier and the crossing point of the two surfaces results (Figure 6). Ideally, when the two potential energy wells are equal in energy the p*K*s are matched and one has the type of identity-proton transfer described above for acetaldehyde-acetaldehyde enolate.[15] The object of this exercise is to match these p*K*s as closely as possible in a system that still exhibits a low activation barrier for α-proton abstraction. These basic concepts have been described earlier in studies on the related TIM catalyzed system.[26] The stronger the H-donors, the less endothermic the reaction (the better pK_a matching), the smaller the barrier and, hence, the earlier the TS. In the absence of the carbonyl H-donors, a reaction with a weakly basic carboxylate will be highly endothermic, the product cluster will be thermodynamically unstable and hence the TS cannot exist.

The formidable ability of the dehydrogenase to stabilize enolate-like species by preferential binding has been noted previously.[1b−d,22a] In this study, we have modeled only the first step of the concerted two-step enzymatic dehydrogenation process executed by acyl-CoA dehydrogenase. Thus, our one-step model reaction is not catalytic in the strictest sense because the overall regeneration of the carboxylate base is not explicitly shown. However, our data are quite consistent with the basic concepts of catalytic enzymatic deprotonation. Importantly, the deep well that we describe here *is not a catalytic trap for normal substrates* because they escape via the concerted transfer of a hydride equivalent shown in Scheme 1. Furthermore, migration of the negative charge to the flavin in the TS for this concerted process will sharply weaken these hydrogen bonds between enzyme and thioester allowing efficient product dissociation.[1b] Desolvation of the active site would effect ionization of the GLU376 and regeneration of the carboxylate base completing the enzymatic cycle. Inspection of Figures 1 and 3 suggests that placement of a desolvated anionic base in the reaction cluster and the subsequent reapportionment of negative charge and ionic H-bonding interactions over all cluster species is a key feature of this enolization reaction.

α-Proton Abstraction from the Thioester Model II. *Extended models d, a*, and b*.* As an extension of the above models, we increased the size of the base from acetate anion to the carboxylate anion of one segment of the GLU376 protein fragment. This is obviously a more realistic base that also describes the role of intermolecular secondary bonding interactions of the model protein with the substrate. Model thioester **II** has an additional methylene group in the alkyl chain and has a slightly more acidic α-proton (ΔPA = 1.3 kcal/mol, Table 1). We have optimized additionally three transition structures (Figures 7 and 8) and their corresponding ground-state clusters. The main feature of these larger models (**d**, **a***, and **b*)** is that they incorporate the hydrogen donating >N−**H** and the basic $-COO^{\ominus}$ functional groups in a single molecule which more closely resembles the protein environment of the enzyme. When the deprotonation reaction is catalyzed by both amide N−**H**

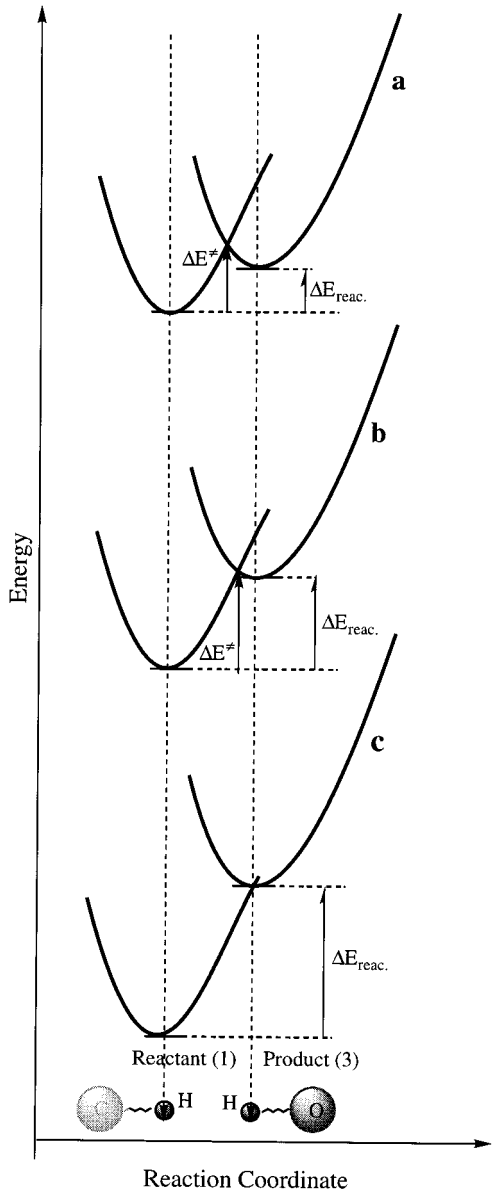

Figure 6. Schematic representation of the activation barrier increase and shift in the position of the transition state (to the product side) in models **a** (two H-donors), **b** (one H-donor) and **c** (no H-donors) for α-proton abstraction by acetate anion from model thioester **I** (CH_3-CH_2(C═O)SCH_3). For each model, two curves describe the potential energy of hydrogen atom vs intranuclear distances H···C and H···O. The reduction of the reaction endothermicity ($\Delta E_{reac.}$) leads to an earlier TS and lower barrier (Hammond postulate). In the case of model **c** (no H-donors), there is no minimum on the product side for this highly endothermic process and, hence, no TS could be located.

and CH_3O-**H** hydrogen donors (model **d**), the activation barrier for α-proton abstraction by the carboxylate is $\Delta E^{\neq} = 7.7$ kcal/mol and the ground state complex is only 4.0 kcal/mol lower in energy (Figure 7). The larger model protein base (H(C═O)−N**H**−$CH_2CH_2CH_2COO^{\ominus}$)) is less basic than acetate anion (ΔPA= 8 kcal/mol, Table 1) reflecting the slightly higher barrier relative to TS-$\mathbf{2_a}$. The N−**H**···O═C H-bond distance is shortened along the reaction coordinate by 0.4 Å reflecting the transfer of negative charge from the carboxylate in the **GS** to the thioenolate fragment in the product complex. The charge on the thioester fragment in TS-$\mathbf{2_d}$ has increased by 0.65 electrons (NBO analysis) with respect to GS complex $\mathbf{1_d}$, but the increase in the charge on the carbonyl oxygen is only 0.09 e. The charge distribution for the overall reaction process provides a rationale for the origin of the phenomenal change in pK_a of the α-proton. In the **GS**, the carboxylate fragment has a charge of −0.96 e, whereas the thioester fragment in the product complex has acquired −0.85 e *most of which resides on the thioester backbone*. Thus, the marked synergy in the H-bond interactions is largely electrostatic in nature. The simple resonance picture of increasing electron density on the enolate oxygen that increases the H-bond strength is clearly not in evidence.

The efficacy of the H-bond donor in catalyzing α-proton removal should be a function of its acidity. Transposition of the N**H** and H(C═O) affords the comparable carboxylate base H(C═O)−CH(NH**H**)$CH_2CH_2COO^{\ominus}$) with the less acidic amine versus an amide as the H-bond donor providing a comparison of the catalytic effect in the TS for α-proton abstraction. As anticipated, in model **a*** the activation energy is increased by 2.2 kcal/mol (TS-$\mathbf{2_{a*}}$, Figure 8). Again, model **b***, as in the above section, does not contain the second H-donor (CH_3O-**H**). The removal of the CH_3O-**H** H-donor molecule in **b*** ($\Delta E^{\neq} = 12.3$ kcal/mol) results in slightly smaller increase ($\Delta\Delta E^{\neq} = 2.4$ kcal/mol) in the barrier in comparison to the smaller model systems ($\Delta\Delta E^{\neq} = 4.5$ kcal/mol for **a** versus **b**). When models **a*** is augmented by one methyl group attached to the >N−**H** functional unit. (**H**N−H vs **H**N−CH_3) the TS comes a little earlier with a shorter C−H distance in the TS (see Supplemental information, Figure S2, TS-$\mathbf{2_a}$). The increase in size of the GLU376 model and junction of the base and hydrogen donor results in an increase in the reaction barriers relative to **a*** ($\Delta E^{\neq} = 9.9$ and 11.3 kcal/mol). The latter barrier for the larger base is in quite good agreement with the experimental barrier of 13 kcal/mol.[1]

The acetate anion used in the smaller model **a** is more basic than the GLU376 model in **d** as indicated by their calculated proton affinities (352.9 vs 345.1 kcal/mol, Table 1). Thus, the overall endothermicity (isolated reactants vs isolated products) is increased to 22.8 kcal/mol in the model **d** (16.3 kcal/mol in the smaller models). The effect of the second H-bond (methanol) to the thioester carbonyl oxygen is an 8.8 kcal/mol decrease in the PA of thioester **II**, and is similar to that of thioester **I** (9.2 kcal/mol, Table 1). By comparison, the H-bond stability for anionic ion−molecule complexes of substituted acetylides with methanol ($RCC^{\ominus}$·$HOCH_3$) are on the order of −21 kcal/mol.[17b] Both hydrogen bonds in model **d** minimize the energy gap between reactant complex ($\mathbf{1_d}$) and product complex ($\mathbf{3_d}$) to 3.7 kcal/mol (Figure 7). Thus, the overall H-bonding contribution to the PA matching in **d** is 19.1 kcal/mol. These combined data provide ample evidence for the catalytic role-played by the H-bond donors in this first step of the enzymatic process.

The protein fragment that serves as the carboxylate base also models the protein backbone atoms and depicts an enzyme-catalyzed reaction. The secondary bonding interactions that holds the pre-reaction complex $\mathbf{1_d}$ together also prevents heavy atom motion. For example, the distance between the carbon atom of the key α-CH_2 group in thioester and the carboxylate carbon atom in TS-$\mathbf{2_d}$ only increases by 0.1 Å relative to reactant complex $\mathbf{1_d}$. The distance between the carbonyl oxygen of $\mathbf{1_d}$ (|NH···O═C| = 2.3 Å) and the amide nitrogen of the protein fragment decreases by about 0.4 Å along the reaction coordinate. There is, however, a large change in the dihedral angle defining the basic carboxylate oxygen as it aligns itself along the C−H bond axis in the TS for proton abstraction.

Free energy estimations that include thermal corrections and the entropy contribution indicate that $\Delta G^{\neq}$ is always less (0.3−2.5 kcal/mol) than the classical activation barrier $\Delta E^{\neq}$ (Table

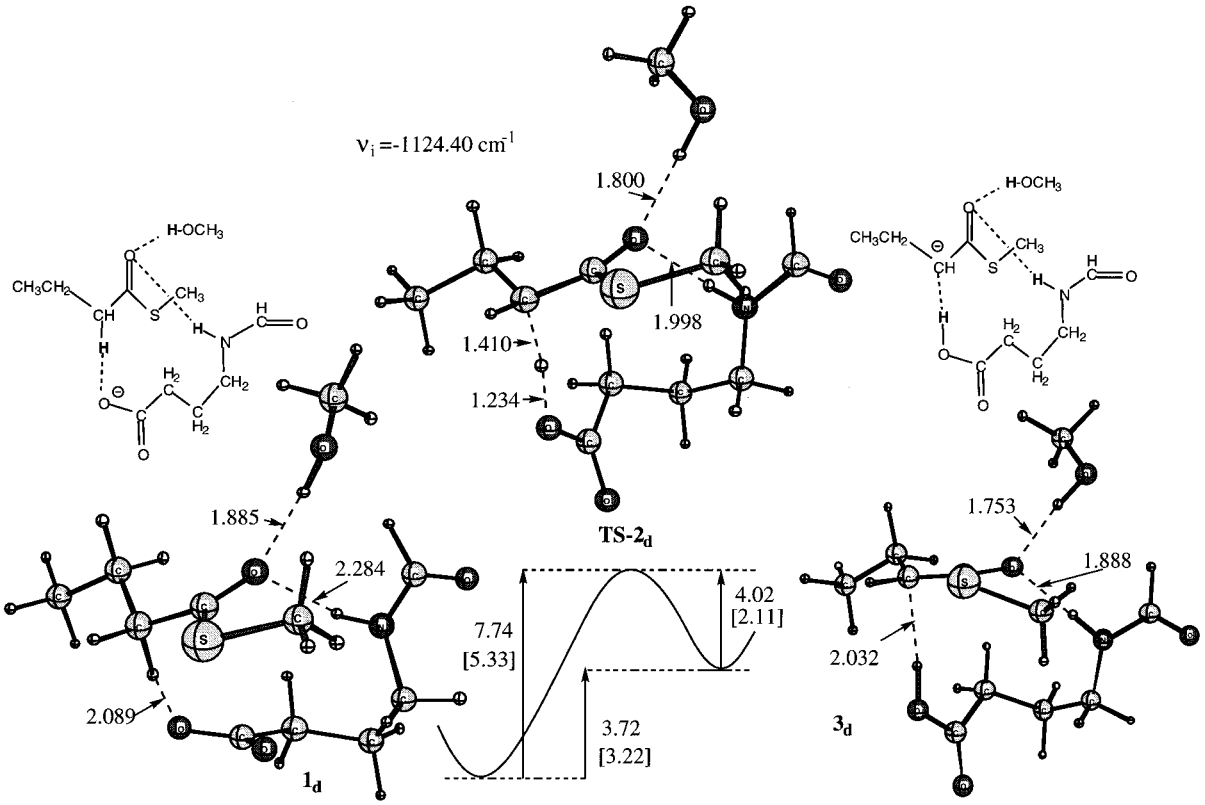

Figure 7. Fully optimized transition structure and relative energies (kcal/mol) of the optimized pre-reaction cluster for thioester **II**, the TS and product cluster of model system **d** ($CH_3CH_2CH\mathbf{H}(C{=}O)SCH_3{\cdot}(CH_3O\mathbf{H}$, ($H(C{=}O){-}N\mathbf{H}{-}CH_2CH_2CH_2COO^{\ominus}$)) at the B3LYP/6-31+G(d,p) level of theory. Numbers in brackets are based upon free energy data. The reactant cluster $\mathbf{1_d}$ has been optimized until the forces, but not displacements, were fully converged.

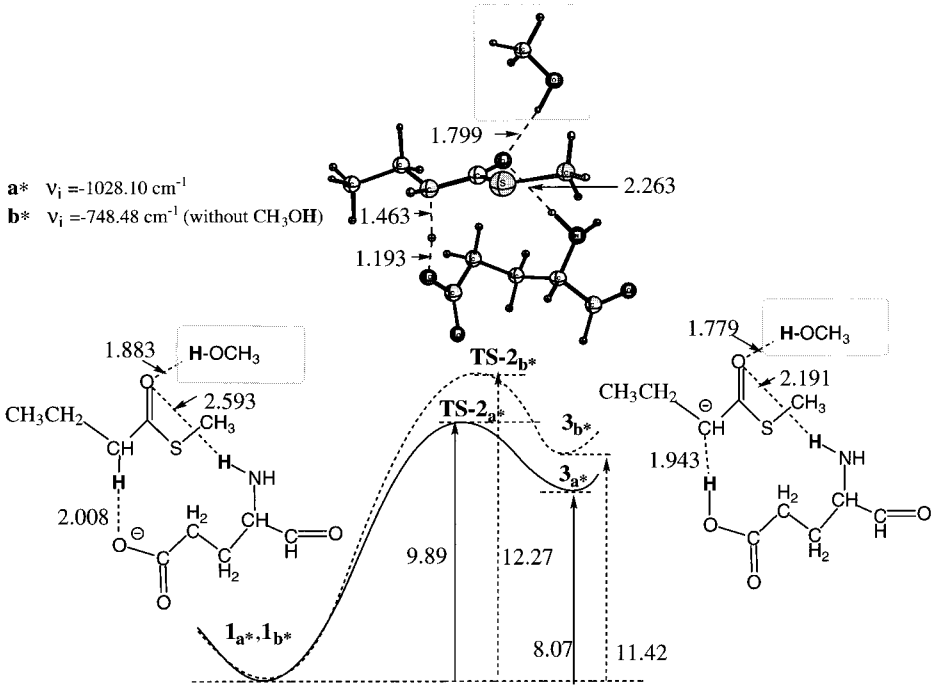

Figure 8. Fully optimized transition structure **TS-2$_a$*** and relative energies (kcal/mol) of the optimized pre-reaction cluster, TS and product cluster of model system **a*** ($CH_3CH_2CH\mathbf{H}(C{=}O)SCH_3{\cdot}(CH_3O\mathbf{H}$, $H(C{=}O){-}CH(NH\mathbf{H})CH_2CH_2COO^{\ominus}$)) and system **b*** (without methanol molecule, $CH_3{-}CH\mathbf{H}(C{=}O)SCH_3{\cdot}$ $H(C{=}O){-}CH(NH\mathbf{H})CH_2CH_2COO^{\ominus}$) at the B3LYP/6-31+G(d,p) level of theory. Bond distances are given for system **a***.

4). The activation entropy ($\Delta S^{\neq}$) varies from −10 to −1 e.u. All of these relatively small entropy contributions are in the range of 1−3 kcal/mol, which is comparable with the accuracy of the method used in this study. It is interesting to note that the imaginary frequency in the TS's without the methanol donor molecule, in contrast to models with two H-bonds to the carbonyl oxygen, is always less than 1000 cm^{-1}. This again indicates an important role of the second H-donor molecule in positioning the TS earlier (higher frequency) on the reaction coordinate.

TABLE 5: Solvent Effects on the Reaction Energetics in Model Systems a, b, d, a*, and b* Calculated at the COSMO//B3LYP/6-31+G(d,p) Level of Theory

structure	$E_{rel.}$, gas phase	$E_{rel.}$, cyclohexane, ϵ=2.02	$E_{rel.}$, aniline, ϵ=6.89	$E_{rel.}$, water, ϵ=78.39
1$_a$	0	0	0	0
TS-2a	5.8	9.9	12.9	16.2
3$_a$	2.4	7.2	10.7	14.7
1$_b$	0	0	0	0
TS-2b	10.4	12.3	14.2	16.9
3$_b$	9.7	12.0	14.1	16.7
1$_d$	0	0		
TS-2d	7.7	11.1		
3$_d$	3.2	8.3		
1$_a$*	0	0	0	
TS-2a*	9.9	14.4	17.8	
3$_a$*	8.1	13.3	17.1	
1$_b$*	0	0	0	
TS-2b*	12.3	17.0	20.4	
3$_b$*	11.4	16.1	19.8	

[a] Relative energies are in kcal/mol.

Estimation of the Solvent Effect on α-Proton Abstraction. The presence of water molecules and their role at the active site of the enzyme catalyzed α-proton abstraction is a matter of considerable discussion.[27] Our model studies are more consistent with the suggestion that displacement of water molecules must precede the key proton abstraction step.[28] Because GLU376 is a relatively weak base it seems logical that it would be desolvated before the deprotonation step involving a weak carbon acid. The basicity of the carboxylate is greatly increased as it approaches a "naked anion" upon desolvation and this is likely the process by which the p*K* of GLU is increased by some 7 p*K* units. For example, the PA of acetate anion is reduced by 11.2 kcal/mol by the inclusion of just one H-bonded water molecule ($CH_3COO^{\ominus}\cdot H_2O$, Table 1). In Table 5 we summarize the solvent effect estimates (COSMO//B3LYP/6-31+G(d,p)) on the reaction energetics in four model systems **a**, **b**, **a***, **b***, and **d**.

These data clearly indicate that an increase in polarity will *increase* the reaction barrier. Thus, in a more polar environment, the ground state pre-reaction complex could experience greater stabilization than the corresponding TS or product complex. However, we are aware of the potential effects of local charged residues not directly involved in the reaction, as well as water molecules, and we are going to extend our studies to more complex and comprehensive models.

4. Conclusions

These calculations provide a quantitative rationalization for why such weak bases as carboxylate anions are thermodynamically incapable of abstracting a proton adjacent to a carbonyl functionality either in the gas phase or in solution. Comparable enzymatic α-deprotonation requires both desolvation of the base GLU376, to increase its basicity, and stabilization of the product cluster by hydrogen bonding at the carbonyl oxygen. Our computational results also suggest that placement of a desolvated anionic base in the reaction cluster and the subsequent reapportionment of negative charge and ionic H-bonding interactions over all cluster species is a key feature of this enolization reaction. This provides a match of the pK_a[28a,b] and decrease in the reaction endothermicity that, in line with the Hammond postulate, results in the lowering of the reaction barrier. The electronic and geometric features of fully optimized transition structures (first-order saddle point) indicate their enolate-like character and that there is no significant increase in charge concentration on the carbonyl oxygen of the enolate. The overall conclusion is that the carbonyl oxygen is not markedly affected by αC−H abstraction in either the simple thioester or when it is hydrogen bonded to two acceptors. Examination of the charge data for transition structure TS-**2$_a$** shows that the increase in the negative charge at the carbonyl oxygen remains at about 10−13% of the total charge shifted. The major portion of charge increase (≥50%) resides on the developing carbanionic center. The carbonyl carbon remains almost unchanged throughout and the SCH_3 group acquires about 20% of the developing negative charge. The C−O bond lengths are changed only minimally, whereas the C−C bond length is intermediate between a single and double bond as would be anticipated for a developing enolate anion. *There is no significant alteration in the geometry and charge distribution that is dependent on the hydrogen bonding interactions.* In sum, these studies support the importance of electrostatic interactions[24b,28c,19] in the stabilization of enolate species within the active center of the dehydrogenase.

One of the more interesting recent developments in enzymology[5] is the realization that hydrogen bonds of the oxygen of the carbonyl group to relatively nonacidic C−H bonds (C−H···O═C) represent a hitherto unrecognized, significant contribution in the determination of protein conformation. The magnitude of this interaction (D_e= −4.0 kcal/mol) is about one-half of the strength of the N−H···O═C hydrogen bonding interaction. The model transition structures for α-proton abstraction suggest that the carboxylate not only serves as the base to remove the proton in acyl-CoA dehydrogenase, but as it is desolvated and approaches the CoA substrate it brings a unit of negative charge to the local environment and strengthens the hydrogen bonds to the α-C−H bond (C−H···$^{\ominus}$OOC-). These interactions serve to disperse this negative charge not only in the GS but also in the TS, thereby strengthening the internal H-bonds all along the entire reaction coordinate. The charge-augmented C−H···$^{\ominus}$OOC H-bond identified here would not only orient the general base prior to proton transfer, but also strengthen those H-bonds to the thioester carbonyl oxygen that prove so critical in the acidification of the α-proton and in lowering the energy of the transition state for enolization. The synergy between H-bonding interactions identified here deserves more attention in related enzymatic examples. We have provided the intrinsic gas-phase energetics for the H-bonding contribution to the α-proton abstraction step for this important reaction. It now remains to evaluate the contribution of the FAD isoalloxazine ring in a comparable fashion.

Acknowledgment. Supported by the NSF (CHE-9901661) and NIH (GM26643). We thank the National Centers for Supercomputing Applications (Urbana) and the University of Kentucky (Lexington) for generous amounts of computer time.

Supporting Information Available: Table S1 [total energies (a.u.) of the selected compounds and molecular systems discussed in the paper]. Table S2 (thermochemical data for the reactant, transition and product structures). Table S3-S4 [selected contributing interactions (kcal/mol) between "filled" and "empty" orbitals calculated with the NBO method]. Table S5 [NBO charge distribution (B3LYP/6-31+G(d,p)) in **1$_a$**, **TS-2$_a$** and **3$_a$**]. Table S6 [Cartesian coordinates of the reactant cluster **1$_d$**, **TS-2$_d$** and **3$_d$** optimized at the B3LYP/6-31G+(d,p)]. Figure S1 [charge evolution along with the reaction coordinate on selected atoms and functional parts of the model **a** calculated using ChelpG (MP2/6-31+G(d,p)//B3LYP/6-31+G(d,p))]. Appendix S1 (comparison between ionic >C═O···H−C< hydrogen bond

and its "normal" H-bond in small model molecular systems). This material is available free of charge via the Internet at http://pubs.acs.org.

References and Notes

(1) (a) Schopfer, L. M.; Massey, V.; Ghisla, S.; Thorpe, C. *Biochemistry* **1988**, *27*, 6599. (b) Thorpe, C.; Kim, J.-J. P. *FASEB J.* **1995**, *9*, 719. (c) Rudik, I.; Ghisla, S.; Thorpe, C. *Biochemistry* **1998**, 37, 8437. (d) Engst, S.; Vock, P.; Wang, M.; Kim, J.-J. P.; Ghisla, S. *Biochemistry* **1999**, *38*, 257; and references therein. (e) Johnson, J. K.; Srivastava, D. K. *Biochemistry* **1993**, *32*, 8004.

(2) Lai, M. T.; Li, D.; Liu, H. W. *J. Am. Chem. Soc*. **1993**, *115*, 1619.

(3) Tamaoki, H.; Nishina, Y.; Shiga, K.; Miura, R. *J. Biochem.* **1999**, *125*, 285.

(4) Shan, S. O.; Herschlag, D. *Proc. Natl. Acad. Sci.* **1996**, *93*, 14 474. (b) Gerlt, J. A.; Kreevoy, M. M.; Cleland, W. W.; Frey, P. A. *Chem. Biol.* **1997**, *4*, 259. (c) Cleland, W. W.; Frey, P. A.; Gerlt, J. A. *J. Biol. Chem.* **1998**, *273*, 25 529. (d) Holden, H. M.; Benning, M. M.; Haller, T.; Gerlt, J. A. *Acc. Chem. Res*. **2001**, *34*, 145.

(5) (a) Derewenda, Z.; Lee, L.; Derewenda, U. *J. Mol. Biol.* **1995**, *252*, 248. (b) Wahl, M. C.; Sundaralingam, M. *TIBS* **1997**, *22*, 97. (c) Bella, J.; Berman, H. M. *J. Mol. Biol.* **1996**, *264*, 734. (d) Sharma, C. V. K.; Panneerselvam, K.; Pilati, T.; Desiraju, G. R. *J. Chem. Soc. Perkin Trans. 2* **1993**, 2209. (d) Vargas, R.; Garza, J.; Dixon, D. A.; Hay, B. P. *J. Am. Chem. Soc*. **2000**, *122*, 4750; and references therein. (e) Olson, C. A.; Shi. Z.; Kallenbach, N. R *J. Am. Chem. Soc*. **2001**, *123*, 6451. (f) see also article by M. Rouhi in Chemical and Engineering News, May 8, 2000, p 15.

(6) (a) Frisch, M. J.; Trucks, G. W.; Schlegel, H. B.; Scuseria, G. E.; Robb, M. A.; Cheeseman, J. R.; Zakrzewski, V. G.; Montgomery, J. A., Jr.; Stratmann, R. E.; Burant, J. C.; Dapprich, S.; Millam, J. M.; Daniels, A. D.; Kudin, K. N.; Strain, M. C.; Farkas, O.; Tomasi, J.; Barone, V.; Cossi, M.; Cammi, R.; Mennucci, B.; Pomelli, C.; Adamo, C.; Clifford, S.; Ochterski, J.; Petersson, G. A.; Ayala, P. Y.; Cui, Q.; Morokuma, K.; Malick, D. K.; Rabuck, A. D.; Raghavachari, K.; Foresman, J. B.; Cioslowski, J.; Ortiz, J. V.; Stefanov, B. B.; Liu, G.; Liashenko, A.; Piskorz, P.; Komaromi, I.; Gomperts, R.; Martin, R. L.; Fox, D. J.; Keith, T.; Al-Laham, M. A.; Peng, C. Y.; Nanayakkara, A.; Gonzalez, C.; Challacombe, M.; Gill, P. M. W.; Johnson, B. G.; Chen, W.; Wong, M. W.; Andres, J. L.; Head-Gordon, M.; Replogle, E. S.; Pople, J. A. *Gaussian 98*, revision A.7; Gaussian, Inc.: Pittsburgh, PA, 1998.

(7) (a) Becke, A. D. *Phys. Rev. A* **1988**, *37*, 785. (b) Lee, C.; Yang, W.; Parr, R. G. *Phys. Rev.* **1988**, *B41*, 785.

(8) (a) Becke, A. D. *J. Chem. Phys.* **1993**, *98*, 5648. (b) Stevens, P. J.; Devlin, F. J.; Chablowski, C. F.; Frisch, M. J. *J. Phys. Chem.* **1994**, *80*, 11 623.

(9) Hehre, W. J.; Radom, L.; Schleyer, P. v. R.; Pople, J. A. *Ab Initio Molecular Orbital Theory*; Wiley: New York, 1986.

(10) Pople, J. A.; Head-Gordon, M.; Raghavachari, K. *J. Chem. Phys.* **1987**, *87*, 5968.

(11) (a) Curtiss, L. A.; Raghavachari, K.; Trucks, G. W.; Pople, J. A. *J. Chem. Phys*. **1991**, *94*, 7221.

(12) (a) NBO Version 3.1, Glendening, E. D.; Reed, A. E.; Carpenter, J. E.; Weinhold, F.; (b) Breneman, C. M.; Wiberg, K. B. *J. Comput.Chem.* **1990**, *11*, 361.

(13) Barone, V.; Cossi, M.; Tomasi, J. *J. Comput. Chem.* **1998**, *19*, 404.

(14) (a) Kim, J. J.; Wang, M.; Paschke, R. *Proc. Natl. Acad. Sci.* USA **1993**, *90*, 7523. (b) Djordjevic, S.; Pace, C. P.; Stankovich, M. T.; Kim, J. J. *Biochemistry* **1995**, *34*, 2163. (c) PDB Ref. Code is 3MDE for medium-chain acyl-CoA dehydrogenase and 1BUC for butyryl-CoA dehydrogenase; Berman, H. M.; Westbrook, J.; Feng, Z.; Gilliland, G.; Bhat, T. N.; Weissig, H.; Shindyalov, I. N.; Bourne, P. E. *The Protein Data Bank. Nucleic Acids Research*, **2000**, *28*, 235−242.

(15) (a) Van Verth, J. E.; Saunders, W. H. *Canad. J. Chem.* **1999**, *77*, 810. (b) Saunders, W. H.; Vanverth, J. E. *J. Org. Chem*. **1995**, *60*, 3452. (c) Saunders, W. H. *J. Am. Chem. Soc.* **1994**, *116*, 5400. (d) Bernasconi, C. F.; Wenzel, P. J.; Keeffe, J. R.; Gronert, S. *J. Am. Chem. Soc.* **1997**, *119*, 4008. (e) Bernasconi, C. F.; Wenzel, P. J. *J. Am. Chem. Soc.* **1996**, *118*, 10 494. (f) Bernasconi, C. F.; Wenzel, P. J. *J. Am. Chem. Soc.* **2001**, *123* (10), *2430*.

(16) (a) Perakyla, M. *J. Phys. Chem.* **1996**, *100*, 3441. (b) Perakyla, M. *J. Chem. Soc., Perkin Trans. 2* **1997**, 2185. (c) Perakyla, M. *Phys. Chem. Chem Phys.* **1999**, *1* (24), 5643.

(17) (a) Johnson, C. E.; Sannes, K. A.; Brauman, J. I. *J. Phys. Chem*. **1996**, *100* (21), 8827. (b) Chabinyc, M. L.; Brauman, J. I. *J. Am. Chem. Soc*. **2000**, *122* (22), 5371. (c) Chabinyc, M. L.; Brauman, J. I. *J. Am. Chem. Soc.* **1998**, *120*, 10863.

(18) When strong bases such as hydroxide ion are involved proton abstraction is very exothermic as evidenced by the differences in proton affinities ($PA_{HO^{\ominus}} - PA_{CH2(C=O)H^{\ominus}} = 22.4$ kcal/mol. For example, the reactant cluster of acetaldehyde with hydroxide ion, the TS and the product cluster all exist at the MP2/6-31+G(d) level of theory ($HO^{\ominus} + CH_3(C{=}O)H \rightleftarrows HOH + CH_2(C{=}O)H^{\ominus}$). However, with the introduction of polarization functions (p-orbitals on hydrogen) in the basis set (6-31+G(d, p)) that more accurately describes the H-bonding interactions, this TS no longer exists.

(19) (a) Donini, O.; Darden, T.; Kollman, P. A. *J. Am. Chem. Soc.* **2000**, *122*, 12 270. (b) Kollman, P. A.; Kuhn, B.; Donini, O.; Perakyla, M.; Stanton, R.; Bakowies, D. *Acc. Chem. Res.* **2001**, *34* (1), 72.

(20) (a) Cui, Q.; Karplus, M. *J. Am. Chem. Soc.* **2001**, *123* (10), 2284. (b) Alagona, G.; Ghio, Caterina; Kollman, P. A. *J. Am. Chem. Soc*. **1995**, *117* (39), 9855. (d) Bash, P. A.; Field, M. J.; Davenport, R. C.; Petsko, G. A.; Ringe, D.; Karplus, M. *Biochemistry* **1991**, *30* (24), 5826.

(21) Behnam, S. M.; Behnam, S. E.; Ando, K.; Green, N. S.; Houk, K. N. *J. Org. Chem*. **2000**, *65* (26), 8970.

(22) (a) For a discussion of problems associated with TSs found at the Hartree−Fock level when the product cluster is not stabilized see: Mulholland, A. J.; Richards, W. G. *J. Phys. Chem.* **1998**, *102*, 6635. (b) Mulholland, A. J.; Richards, W. G. *Proteins: Struct., Funct., Genet*. **1997**, *27*, 9. (c) Mulholland, A. J.; Lyne, P. D.; Karplus, M. *J. Am. Chem. Soc.* **2000**, *122*, 534.

(23) Gu, Y.; Kar, T.; Scheiner, S. *J. Am. Chem. Soc*. **1999**, *121*, 9411.

(24) (a)The unstabilized reaction "isolated reactants → isolated products" is endothermic (16.3 kcal/mol [17.0 at the G2 level of theory]). Highly endothermic α-proton abstraction, if it occurs, would come late along the reaction coordinate and the TS would closely resemble the product. The energy of the product cluster $\mathbf{3_c}$ (and of $\mathbf{TS\text{-}2_c}$ as well) was estimated based upon an optimized cluster with fixed O−H = 1.01 Å distance. Similar problem have been found in the vinylglycolate substrate/ethylamine complex: (b) Garcia-Viloca, M.; Gonzalez-Lafont, A.; Lluch, J. M. *J. Am. Chem. Soc.* **2001**, *123*, 709.

(25) Donahue, N. M. *J. Phys. Chem. A.* **2001**, *105* (9), 1489.

(26) Aaqvist, J.; Fothergill, M. *J. Biol. Chem*. **1996**, *271* (17), 10 010.

(27) (a) Sargent, A. L.; Rollog, M. E.; Almlof, J. E.; Gassman, P. G.; Gerltt, J. A. *J. Mol. Struct. (THEOCHEM)* **1996**, *388*, 145. (b) Warshel, A.; Strajbl, M.; Villa, J.; Florián, J. *Biochemistry* **2000**, *39* (48), 14 728. (c) Strajbl, M.; Florián, J.; Warshel, A. *J. Am. Chem. Soc*. **2000**, *122*, 5354.

(28) (a) Gerlt, J. A.; Gassman, P. G. *J. Am. Chem. Soc.* **1993**, *115*, 11 552. (b) Gerlt, J. A.; Gassman, P. G. *Biochemistry* **1993**, *32*, 11 943. (c) Kozarich, J. W.; Gerlt, J. A.; Kenyon, G. L.; Gassman, P. G. *J. Am. Chem. Soc.* **1991**, *113*, 9667 (d) Warshel, A.; Papazyan, A.; Kollman, P. A. *Science* **1995**, *269*, 102.